TECHNICAL MEMORANDUM

X-810

THE EXPLORER XVI MICROMETEOROID SATELLITE

DESCRIPTION AND PRELIMINARY RESULTS FOR THE PERIOD

DECEMBER 16, 1962, THROUGH JANUARY 13, 1963

Compiled by Earl C. Hastings, Jr.

Langley Research Center
Langley Station, Hampton, Va.

NATIONAL AERONAUTICS AND SPACE ADMINISTRATION

WASHINGTON   February 1963

NATIONAL AERONAUTICS AND SPACE ADMINISTRATION

TECHNICAL MEMORANDUM X-810

THE EXPLORER XVI MICROMETEOROID SATELLITE

DESCRIPTION AND PRELIMINARY RESULTS FOR THE PERIOD

DECEMBER 16, 1962, THROUGH JANUARY 13, 1963

Compiled by Earl C. Hastings, Jr.

SUMMARY

Explorer XVI (1962 Beta Chi 1) data that have been analyzed for the period between December 16, 1962 (launch date), and January 13, 1963, indicate that the orbit achieved was close to the predicted orbit.

Ten punctures of annealed 0.001-inch-thick beryllium-copper have been used to determine a puncture rate of 0.035 per square foot per day in this material. One puncture of a 0.002-inch-thick sample has also occurred in this period. A tentative evaluation of the puncture rate for the 0.001-inch beryllium-copper in terms of the rate for an equivalent thickness of aluminum has been attempted, and the result has been compared with two different puncture rate estimates.

The three micrometeoroid impact detecting systems are operating. Counting rates for the high- and low-sensitivity systems were close to anticipated values near the end of 1 week.

Two of the 0.001-inch-steel-covered grid detectors have been punctured, but none of the 0.003- or 0.006-inch-steel-covered grid detectors have indicated punctures. One of the cadmium sulfide cells indicates three punctures of the 0.00025-inch Mylar cover. None of the 0.002- or 0.003-inch-copper-wire cards have indicated a break in the period covered.

Telemetry temperatures were initially higher than expected although they remained well within operating limits. Sensor temperatures have remained within the expected bounds.

INTRODUCTION

Explorer XVI (1962 Beta Chi 1, also designated the S-55B micrometeoroid satellite) is part of a micrometeoroid program being directed by the National Aeronautics and Space Administration Office of Advanced Research and Technology

and is managed by the Langley Research Center. The satellite was placed in orbit on December 16, 1962, by the Scout launch vehicle.

There are three major objectives of the experiment. The first is to obtain a direct measure of the micrometeoroid puncture hazard in thin samples of several materials. The second objective is to obtain additional data on meteoroid impacts having insufficient energies to puncture the thinnest of the sensors. The momentum sensitivity ranges were selected so as to provide information in the ranges where little data exist, and possibly provide correlation of microphone impact rates with puncture rates. The third objective is to obtain solar-cell degradation data for various solar-cell protective arrangements.

The purpose of this report is to present some of the more important data obtained during the first 4 weeks of operation of Explorer XVI. In order to expedite publication of this initial report, data that have not been completely reduced have been omitted. The report is thus preliminary in nature. It is being distributed at this time in order to provide spacecraft designers with the available data. Supplementary reports will be prepared as further significant data become available.

The various parts of the Explorer XVI program are under several different experimenters and specialists, who have also contributed much of the text in this report relating to their particular areas. These experimenters and specialists are listed in the following tabulation, together with their research centers and the parts of the program with which they are involved. Mr. Earl C. Hastings, Jr. is project manager.

Contributor	Area
Alfred G. Beswick Langley Reaearch Center	Meteoroid Impact Detection Systems
Elmer H. Davison Lewis Research Center	Steel-Covered Grid Detectors
Charles A. Gurtler Langley Research Center	Pressurized-Cell Experiment
Earl C. Hastings, Jr. Langley Research Center	Orbital Elements Temperatures
William H. Kinard Langley Research Center	Conversion Factor (Be-Cu to Al)
Sheldon Kopelson Langley Research Center	Data Reduction
Walt C. Long Langley Research Center	Telemetry System
John L. Patterson Langley Research Center	Power Supplies and Test Solar Cells
Luc Secretan Goddard Space Flight Center	Cadmium Sulfide Cells Copper-Wire Card Detectors

DESCRIPTION OF SPACECRAFT AND EXPERIMENTS

Figure 1(a) is a sketch of the Explorer XVI; figure 1(b) is a photograph showing the spacecraft with antennae extended. The satellite is cylindrical in shape and is approximately 23 inches in diameter and 76 inches long. It was built around the fourth-stage motor of the launch vehicle, and the burned-out last-stage motor remained as part of the orbiting satellite. Five types of sensors are used to obtain information regarding micrometeoroids. These sensors, as noted in figure 1(a), are impact detectors and cadmium sulfide cells on the nose cone, pressurized cells, additional impact detectors mounted on the base plate of some of the pressure cells, stainless-steel-covered grid detectors, and copper-wire card detectors. These experiments are discussed in more detail in the following paragraphs.

The pressurized cells, developed at the Langley Research Center, are the primary experiment. Figure 2 is a drawing of the pressurized-cell detector. A total of 160 of the annealed beryllium-copper cells are mounted around the periphery of the rocket motor case in 5 rows of 32 cells each. Each cell is filled with helium; when the cell is punctured, the gas leaks out and the pressure loss actuates a switch that signals the telemeter of the puncture. Thus, after one puncture, the cell cannot indicate additional punctures.

A cross-sectional view of some of the pressure cells mounted around the periphery of the satellite is shown in figure 3. Radii from the axis of symmetry of the satellite to the external surface of the cells and to the mounting surface of the cells are shown, as well as the spacing between the cells. There is an 0.08-inch gap between adjacent cells, except for four 0.44-inch gaps equally spaced around the periphery of the satellite for antenna storage during the launching. Each cell has a total sensitive area of 0.151 square foot.

The area exposed to the influx of micrometeoroids in space is considered to be π times the diameter to the outer surface (23 inches, see fig. 1), multiplied by the detector sensing length of the column of five detectors (35.6 inches) with some correction for the open area between the sensors. This definition of area yields a total value of 17 square feet for the prelaunch condition. In this paper, all areas connected with the pressure-cell experiment will be based on this concept. The areas corresponding to the various thicknesses are listed in the following table:

Table I

External skin thickness, in.	Number of cells	Area, sq ft
0.001	100	10.625
.002	40	4.250
.005	20	2.125

3

The material was specified to have a tolerance of ±0.0002 inch. Examination of the material received indicated that the deviation of thickness from the nominal value ranged from 0.0000 to +0.0003 inch.

The second type of sensor is the stainless-steel-covered grid detector developed by the Lewis Research Center. Sensors made of type 304 stainless-steel segments were mounted around the base of the fourth-stage motor. Each segment has an area of 9 square inches and is mounted to the outside surface of a thin continuous grid circuit. (See fig. 4.) A puncture of the stainless-steel cover will break the circuit beneath it, and is indicated by a change in resistance. Thicknesses and areas of these segments are listed in the following table:

Table II

Channel number	Material thickness, in.	Number of sensors	Area per sensor, sq in.	Total area, sq ft
1	0.001	8	[a]18	1.0
2	.001	8	9	.5
3	.003	8	[a]18	1.0
4	.003	8	9	.5
5	.003	[b]8	9	.5
6	.006	4	9	.25

[a]These are actually two 9-square-inch segments connected in series, so that one puncture of either segment eliminates both segments.

[b]One sensor on this channel indicated a break prior to lift-off.

Figure 5 shows a sensor of the type developed by the Goddard Space Flight Center. Forty-six of these copper-wire cards are mounted on a cylindrical structure aft of the steel-covered grids. Each card consists of a continuous winding of 0.002- or 0.003-inch copper wire closely wound on a melamine card. The area wound is 0.0474 square foot for each card. Each 0.002-inch card forms a separate sensor, but the 0.003-inch sensors are formed from two cards in series. Sensor operation is similar to that of the steel-covered grids in that a puncture, or break, of the wire causes a change in circuit resistance. These sensors, as well as the two types of puncture sensors previously described, cannot provide additional data once a puncture has occurred. Wire thicknesses and areas of the wire cards are listed in the following table:

Table III

Diameter of copper wire, in.	Number of sensors	Area per sensor, sq ft	Total area, sq ft
0.002	14	0.0474	0.664
.003	16	.0948	1.517

Impact detectors of three levels of momentum sensitivity were developed for Explorer XVI at the Langley Research Center. Two acoustically isolated "sounding boards" on the nose cone are used for the highest and lowest levels, and the twenty 0.005-inch pressure cells are instrumented with transducers for the intermediate sensitivity level. Figures 6 and 7 are drawings of the impact detectors on the sounding boards and pressure cells. The following table lists the areas and design sensitivities of the impact detectors:

Table IV

Component	Total area, sq ft	Design sensitivity
Sounding boards	1.53	$\begin{cases} 1 \text{ dyne-sec} \\ .01 \text{ dyne-sec} \end{cases}$
0.005-inch pressure cells	2.30	.1 dyne-sec

It should be noted that the pressurized-cell area listed is not the same as that of table I. The reason is that the sensitive areas are not the same, since the overhanging edges are sensitive to impacts but not to punctures.

Each of the two sounding boards is sensitized to impact by a pair of piezoelectric crystals, mounted on its underside and electrically paralleled. The impact event signals from both sounding boards are sent to an amplifier, which equalizes the effective sensitivity of the two sounding boards. The two sounding boards, in effect, thus function as one transducer, and the high- and low-sensitivity threshold levels are selected electronically.

The fifth type of micrometeoroid sensor used on this satellite is shown in figure 8. This is the cadmium sulfide cell developed by the Goddard Space Flight Center. It consists of a light-sensitive cadmium sulfide element mounted beneath a sheet of 0.00025-inch Mylar with vapor-deposited aluminum on both sides. The purpose of the experiment is to determine the size of the hole left in the Mylar by a penetrating particle, by measuring the change in resistance caused by the sunlight admitted through the hole. Two of these cells, with a total exposed area of 7.52 square inches, are mounted on the nose cone.

As mentioned in the Introduction, the third objective of the satellite is to gather data useful in evaluating solar-cell degradation. Five groups of test solar cells with various shielding are mounted on the nose cone. The output of each group of cells is telemetered. All cells are of the p-on-n type and have nominal efficiencies of 8 percent. Details of the shielding are given in the following table:

TABLE V

Test solar-cell group	Cover	Cover thickness, in.
1	Uncovered	
2	Glass slide bonded to cell	0.006
3	Fused silica	.188
4	Glass slide bonded to cell	.006
5	Glass slide bonded to cell	.006

The primary test solar-cell groups (1 to 3) are mounted on the forward face of the nose cone, and test solar-cell groups 4 and 5 are mounted 180° apart on the cylindrical section of the nose cone between the power solar cells. In addition to voltage, which is monitored on all test solar cells, temperatures were also measured on groups 1 to 3. Figure 9 is a sketch of the solar-cell arrangement for groups 4 and 5.

TELEMETRY SYSTEM

The telemetry system for the Explorer XVI consisted of two separate and independent telemeters for telemetering the data and a radio beacon for initial tracking of the satellite. The two telemeters are of the data-storage, command readout type wherein data are collected during the satellite's orbit(s) and read out when within range of a Minitrack data-acquisition station. Data storage is sufficient to allow up to 24 hours to elapse between readouts even during meteoroid shower activity. Data readout is nondestructive so that noisy receptions can be discarded and the readouts repeated later. It was necessary to use two radio-frequency links for data transmission, but only one command frequency is used for commanding the readout.

The two telemeters are constructed as independently as possible in order to provide telemetry redundancy and thus improve overall system reliability. Separate solar cells and batteries are used to supply power to each telemeter. Redundancy is provided in the command system by connecting the two command receivers so that either command receiver can turn on both telemeters. A common antenna system is used for both telemeters, but the two telemeters are connected through a hybrid junction so as to be electrically isolated. The various sensors are divided into two groups as nearly equal as possible and are telemetered separately. Any given sensor is connected to one system only so that the same piece

of information is telemetered only once, but the division is made so that the same types of information are transmitted by both systems. Accordingly, if one telemeter fails, the entire experiment will not be lost, but the exposed area for each type of experiment will be halved.

The telemetry system is shown in block diagram form in figure 10; the pertinent characteristics are presented in the following table:

Table VI

	Telemeter A	Telemeter B	Radio beacon
Type	PDM/FM/AM 48 channels	PDM/FM/AM 48 channels	MOPA
Emission	30A9 for 1 minute, upon interrogation only	30A9 for 1 minute, upon interrogation only	OAO
Frequency, mcps . . .	136.200	136.860	136.860
Power output, mw . . .	200	200	100
Lifetime, days	Indefinite	Indefinite	15
Power supply	Secondary batteries (Ni-Cd) recharged by solar cells	Secondary batteries (Ni-Cd) recharged by solar cells	Primary batteries (Hg)

The telemetry system consists of three major units: an A telemeter, a B telemeter, and a radio beacon. The telemeter assemblies consist of:

1. One signal conditioning module.
2. One encoder module.
3. One subcarrier oscillator module.
4. One counter in the A unit and two counters in the B unit.
5. One impact detector amplifier module.
6. One transmitter module.
7. One secondary battery (Ni-Cd) module.
8. One command receiver module.
9. One dc-dc converter module.

The modules are stacked one upon another and the two assemblies are referred to as the A and B stacks. The radio beacon consists of:

1. The transmitter in the B stack.
2. Six primary battery (Hg) packs.

ORBITAL ELEMENTS

Presented in the following table is a comparison of some of the predicted orbital elements of Explorer XVI with the measured orbital elements as determined by Goddard Space Flight Center on December 16, 1962 (initial computation), and on January 16, 1963.

Table VII

	Predicted	Measured as of Dec. 16, 1962	Measured as of Jan. 16, 1963
Perigee altitude, km	731.86	750.21	750.19
Apogee altitude, km	1,099.07	1,180.14	1,180.37
Inclination, deg	51.43	52.006	52.004
Period, min	103.2	104.377	104.379
Eccentricity	.02519	.02927	.02929

Additional orbital elements measured as of January 16, 1963, are as follows:

Table VIII

Semimajor axis, earth radii	1.15133
Mean anomaly, deg	349.618
Right ascension of ascending node, deg	10.779
Velocity at perigee, km/hr.	27,312
Velocity at apogee, km/hr	25,758
Geocentric latitude of perigee, deg	-13.116

PRESSURIZED-CELL EXPERIMENT

Results

Data have been reduced from 26 interrogations, the last of which was on the 391st pass. Table IX shows a time history of the interrogations and results. During the first 28 days of orbital lifetime, ten 0.001-inch and one 0.002-inch detectors were punctured.

The area exposed to the influx of micrometeoroids in space was considered to be π times the diameter shown in figure 1 times the detector sensing length of a column of detectors with some correction for the open area between the detectors. The area of the experiment is thereby considered to be 17 square feet.

Table IX

Pass	Greenwich date	Greenwich mean time at interrogation	Accumulated punctures for detector thickness of -		
			0.001 in.	0.002 in.	0.005 in.
Lift-off	Dec. 16, 1962	14:33	0	0	0
1	Dec. 16, 1962	16:26	0	0	0
10	Dec. 17, 1962	07:39	0	0	0
11	Dec. 17, 1962	09:33	0	0	0
13	Dec. 17, 1962	13:05	0	0	0
14	Dec. 17, 1962	14:53	0	0	0
23	Dec. 18, 1962	06:09	0	0	0
25	Dec. 18, 1962	09:48	0	0	0
27	Dec. 18, 1962	13:27	0	0	0.
28	Dec. 18, 1962	15:23	0	0	0
39	Dec. 19, 1962	10:10	0	0	0
40	Dec. 19, 1962	12:00	0	0	0
41	Dec. 19, 1962	13:49	0	0	0
53	Dec. 20, 1962	10:33	0	0	0
54	Dec. 20, 1962	12:23	1	0	0
55	Dec. 20, 1962	14:11	1	0	0
66	Dec. 21, 1962	09:06	1	0	0
68	Dec. 21, 1962	12:44	1	0	0
79	Dec. 22, 1962	07:39	2	0	0
81	Dec. 22, 1962	11:17	2	0	0
96	Dec. 23, 1962	13:35	3	0	0
105	Dec. 24, 1962	04:43	4	0	0
137	Dec. 26, 1962	12:53	5	0	0
206	Dec. 31, 1962	12:47	5	0	0
259	Jan. 4, 1963	08:55	6	0	0
378	Jan. 12, 1963	23:26	10	1	0
391	Jan. 13, 1963	21:59	10	1	0

Data reduction has not been completed for any of the passes between January 4 and January 12 so that the exact dates of the punctures during this interval are not known. The area of the experiment is reduced each time one of the sensors is punctured. Equal increments of time have been assumed between the new punctures read out on January 12 for the purpose of establishing the time-area products during this interval. The time-area products and the puncture rates for the various thicknesses are as follows:

Table X

Material thickness, in.	Number of punctures	Time-area products for first 28 days, (sq ft)(days)	Puncture rate, punctures/sq ft/day
0.001	10	284	0.035
.002	1	119	.008
.005	0	59	

It should be emphasized that the puncture rate for the 0.002-inch sensor is based on one puncture.

Comparison With Predictions

Figure 11 is a plot of the predicted puncture rate as a function of thickness for aluminum sheet, from reference 1. The puncture rate of beryllium-copper, as shown in table X, has been related (by consideration of the factors discussed subsequently) to the estimated rates of puncture in aluminum sheet. This plot compares the Explorer XVI puncture rate with the rates predicted from the Whipple (1961) distribution and the Watson (1956) distribution on the basis of the Bjork penetration theory. This comparison indicates that the Explorer XVI data would lie between the Watson and Whipple curves.

A comparison of the puncture rate obtained on Explorer XVI requires the consideration of earth shielding, the conversion factor between beryllium-copper and aluminum, and impact incidence angle. These factors, as used herein, are discussed in the following sections.

Earth shielding.- The Whipple and Watson flux rates are given in terms of the influx rate to the earth. From the mean altitude of Explorer XVI, one may estimate that the earth shields 1/4 of the 4π-steradian influx of micrometeoroids. In plotting the Explorer XVI data in figure 11, the experimentally indicated influx was accordingly multiplied by 4/3 in order to obtain the comparison with the Whipple and Watson curves.

Conversion factor for relating beryllium-copper skin thickness to that of aluminum.- A brief experimental investigation was made in the hypervelocity impact laboratory at the Langley Research Center to establish the relationship

between impact penetration depths obtained in beryllium-copper targets and penetration depths obtained in aluminum targets under similar impact conditions.

The beryllium-copper targets used were of Berylco No. 25, solution annealed to a hardness of B-60. This material is the same alloy with approximately the same heat treatment as that used for the pressurized cells on the Explorer XVI. The beryllium-copper targets were all thick enough to behave under impact as quasi-infinite blocks of material.

The aluminum targets used in the investigation were all 2024-T3 aluminum-alloy blocks, also thick enough to behave as quasi-infinite blocks of material.

Spherical projectiles 1/16 inch in diameter were fired against the targets of both materials. The projectiles were made of aluminum, copper, and steel. They were fired from a 22-caliber light-gas gun against the targets in a vacuum chamber. The spheres were mounted on magnesium sabots during launch from the gun. After launch, the sabots were deflected from the flight path of the sphere. Impact velocities approaching 17,000 feet per second were obtained.

The results of this investigation indicate that under similar impact conditions the penetration depths in aluminum targets will be approximately twice the penetration depths in beryllium-copper targets. This fact is illustrated by the data presented in figure 12.

In figure 12 the penetration depths of aluminum projectiles striking both beryllium-copper and aluminum targets were plotted against the impact velocity. The upper line faired through the aluminum-target data has twice the slope of the line faired through the beryllium-copper-target data.

The data obtained with the copper and steel projectiles have also shown the penetration depths in the aluminum targets to be twice the depths in the beryllium-copper targets at any given impact velocity.

The impact conditions achieved in this investigation obviously do not simulate micrometeoroid impacts in space; however, in the absence of more appropriate data, it is assumed that the trends observed in this investigation are preserved under meteoroid impact conditions.

Incidence angle.- The incidence angle at which the micrometeoroid strikes the sensor will affect the thickness of the material penetrated. In reference 2, the crater depth was found to depend on the velocity component normal to the surface, for semi-infinite targets. However, no correction for this effect has been made in the Explorer XVI puncture rate plotted in figure 11.

STEEL-COVERED GRID DETECTORS

To date this experiment appears to be operating satisfactorily and as predicted. Data received through the 391st pass (taken 703.5 hours after lift-off) indicate that two of the 0.001-inch-stainless-steel sensors have been

punctured. These punctures are on channels 1 and 2. (See table II.) Prior to launch, a break in the 0.003-inch sensors in channel 5 was indicated, so there should be a corresponding reduction in the initial area exposed for channel 5.

COPPER-WIRE CARD DETECTORS

In the period covered by this report, there have been no breaks in either the 0.002- or the 0.003-inch-copper-wire cards.

CADMIUM SULFIDE CELLS

Three punctures have occurred in the shield of one of the cadmium sulfide cells between December 16, 1962, and January 13, 1963. No punctures have occurred in the shield of the second cadmium sulfide cell. Analysis of these data to evaluate time of occurrence and hole size is being conducted, but is not complete enough at this time to be included in this report.

METEOROID IMPACT DETECTION SYSTEMS

The three impact detection systems appear to have operated satisfactorily during the period covered by this report. Examination of the limited amount of data that have been reduced to date shows that the counting rates of the high- and low-sensitivity systems were close to what was anticipated by the end of the first week in orbit (pass number 105). However, since some of the necessary corrections to the impact data have not as yet been made, no counting rates are presented in this report.

POWER SUPPLIES AND TEST SOLAR CELLS

Telemetered values of battery voltages indicated that the power supplies were still functioning normally as of January 13, 1963.

Not enough data have yet been reduced to permit an accurate determination of the degradation of the test solar cells at this time.

TELEMETRY PERFORMANCE

Telemetry data taken before and after launch indicate that all systems were injected into orbit without suffering any damage. One steel-covered grid sensor was open, but this condition was known for some time prior to launch. The latest

12

available data, taken at 21:59 Greenwich mean time on January 13, 1963, also indicate all systems functioning with data coming in.

A special station was set up at Antigua, British West Indies, to obtain an early interrogation and establish puncture references at injection into orbit. Although Antigua was able to make a successful command, an antenna malfunction at the station became evident and no data were recorded at Antigua. However, since the command from Antigua did turn on the telemetry, the backup station at Fort Myers, Florida, was able to record weak but usable signals which verified that no sensor damage had occurred during ascent.

The radio beacon, which was used to establish the orbital track, functioned properly throughout its lifetime. Performance was such that Goddard Space Flight Center was able to issue preliminary orbital elements 6 hours and 9 minutes after lift-off. The radio-beacon power supply had been designed for a minimum lifetime of 15 days; the radio beacon actually transmitted for about 20 days.

The sensitivity of the command system in Explorer XVI had been increased over that previously employed in Explorer XIII (1961 Chi), because of difficulties experienced in commanding Explorer XIII. This increase resulted in the command system being somewhat more subject to spurious commands. Some responses to spurious commands have occurred, but, because of the fail-safe nature of the telemetry system (nondestructive readout and automatic reset), no data have been lost.

TEMPERATURES

A great deal of the Explorer XVI temperature data has not yet been fully analyzed. For this reason, only telemetry temperature variation with time is plotted in this report. Other temperatures (sensors, solar cells, etc.) will be given herein only as bands defining the maximum and minimum values recorded. A complete evaluation of these surface temperatures must consider such factors as heating sources, time of interrogation, spacecraft attitude, and spin mode.

Figure 13 is a plot of telemetry temperature as a function of hours after launch. These values of temperature were measured by thermistors placed in both encoder modules of the two telemeters (A and B telemeter stacks). The accuracy of these data is approximately $\pm 5^{\circ}$ F.

Telemetry temperatures on both stacks were considerably higher than expected during the first 450 hours, with the B stack temperature consistently higher than the A stack temperature. During this time the satellite was spinning about its longitudinal axis and the radio beacon was operative. The data available after 655 hours, when the satellite was essentially tumbling and the beacon was dead, show that the A and B stack temperatures are in better agreement and have decreased to a value very near the expected temperature. Studies are under way to evaluate the cause of the earlier elevated temperatures.

13

The following table lists the highest and lowest temperatures recorded on other parts of the spacecraft after the dissipation of the heat associated with the ascent:

Table XI

Component	Highest temperature, °F (a)	Lowest temperature, °F (a)
Cadmium sulfide cells	111	77
Pressure cells	84	29
Grid detectors	40	-20
Wire card detectors	58	-20
Power solar cells	75	16

[a]These are the highest and lowest temperatures found in the records reduced in the period covered by this report.

Although the range is large in some cases, it must be remembered that external surface temperatures are strongly influenced by the time of interrogation (daylight or darkness) so that fluctuations are to be expected. These ranges are quite reasonable in light of the thermal design calculations and indicate that, after dissipation of the heat associated with the ascent, the coatings used are providing the proper surface temperatures.

Two sources of heat can be directly attributed to the ascent environment. These are the inside wall of the vehicle heat shield and the hot rocket-motor case. Reference 3 contains detailed descriptions and analyses of these heating effects. These effects were most evident in the pressure-cell temperature, which was 109° F on the first pass, and in the temperature of the steel-covered grids, which was 83° F on the first pass. Other external surface temperatures were generally less than the lift-off temperature at the first interrogation.

DATA REDUCTION

The telemetered data from the Explorer XVI were reduced at the Langley Research Center. An automatic PDM-PFM data readout system, developed at this Center, is used to decommutate and digitize the telemetry signals, which are recorded on magnetic tape at the various stations of the Minitrack network of the Goddard Space Flight Center. The digital output of the readout system is recorded on magnetic tape in the format for the IBM 7070 electronic data processing system. The results of the data processing are tabular listings of the physical quantities measured by each experiment.

A detailed analysis has been made of previously processed Explorer XIII data to determine the scatter error of the read out data as a function of the signal-to-noise ratio of the received telemetry signal. From this study, it has been concluded that for signal-to-noise ratios above 11 decibels, the standard deviation of the time-coded data can be expected to be less than 1.5 percent of full scale. Similarly, the standard deviation of the frequency-coded data can be expected to be less than 3 percent of full scale. The signal-to-noise ratios of the Explorer XVI telemetry data processed to date are estimated to be greater than 11 decibels. A minimum of 20 points per channel are read out for each processed interrogation of the Explorer XVI satellite; thus, increased reliability in the mean values of the measured physical quantities is provided.

Correlation of the data with the orbital position of the satellite is provided through readout of the serial-coded Greenwich mean time, which is recorded on one track of the telemetry tape.

CONCLUDING REMARKS

Between the launch data, December 16, 1962, and January 13, 1963, all systems and experiments on Explorer XVI have functioned properly, and it appears that the mission of the satellite is being successfully fulfilled. An orbiting lifetime well in excess of that required to perform the mission is indicated.

The puncture rate in annealed 0.001-inch beryllium-copper sheet, derived on the basis of the 10 punctures received to date, is 0.035 puncture/sq ft/day. One puncture of a 0.002-inch cell occurred in the period covered by this report.

A tentative conversion of this puncture rate for 0.001-inch beryllium-copper to that for an equivalent thickness of aluminum has been attempted, and the result has been compared with two previous estimates of puncture rates. The comparison indicates that the Explorer XVI data lie between the two estimates.

Two of the 0.001-inch-steel-covered grid detectors have been punctured, and the shield of one of the cadmium sulfide cells has been punctured three times. None of the 0.002- and 0.003-inch-copper-wire cards have indicated a break in the period covered.

The limited amount of temperature data analyzed indicates that, although telemetry temperatures were well within operating limits, they were higher than expected for about the first 3 weeks. Temperatures of the sensors and solar cells have been quite close to the expected values.

Langley Research Center,
    National Aeronautics and Space Administration,
   Langley Station, Hampton, Va., February 7, 1963.

REFERENCES

1. Davidson, John R., and Sandorff, Paul E.: Environmental Problems of Space
   Flight Structures - II. Meteoroid Hazard. NASA TN D-1493, 1963.

2. Summers, James L.: Investigation of High-Speed Impact: Regions of Impact
   and Impact at Oblique Angles. NASA TN D-94, 1959.

3. Hastings, Earl C., Jr., Turner, Richard E., and Speegle, Katherine C.:
   Thermal Design of Explorer XIII Micrometeoroid Satellite. NASA TN D-1001,
   1962.

Solar-cell test trays

Solar cells

Impact detector

Cadmium sulfide cell

Solar cells

Pressure cells

22.98 inch diameter

Grid detector

Wire cards
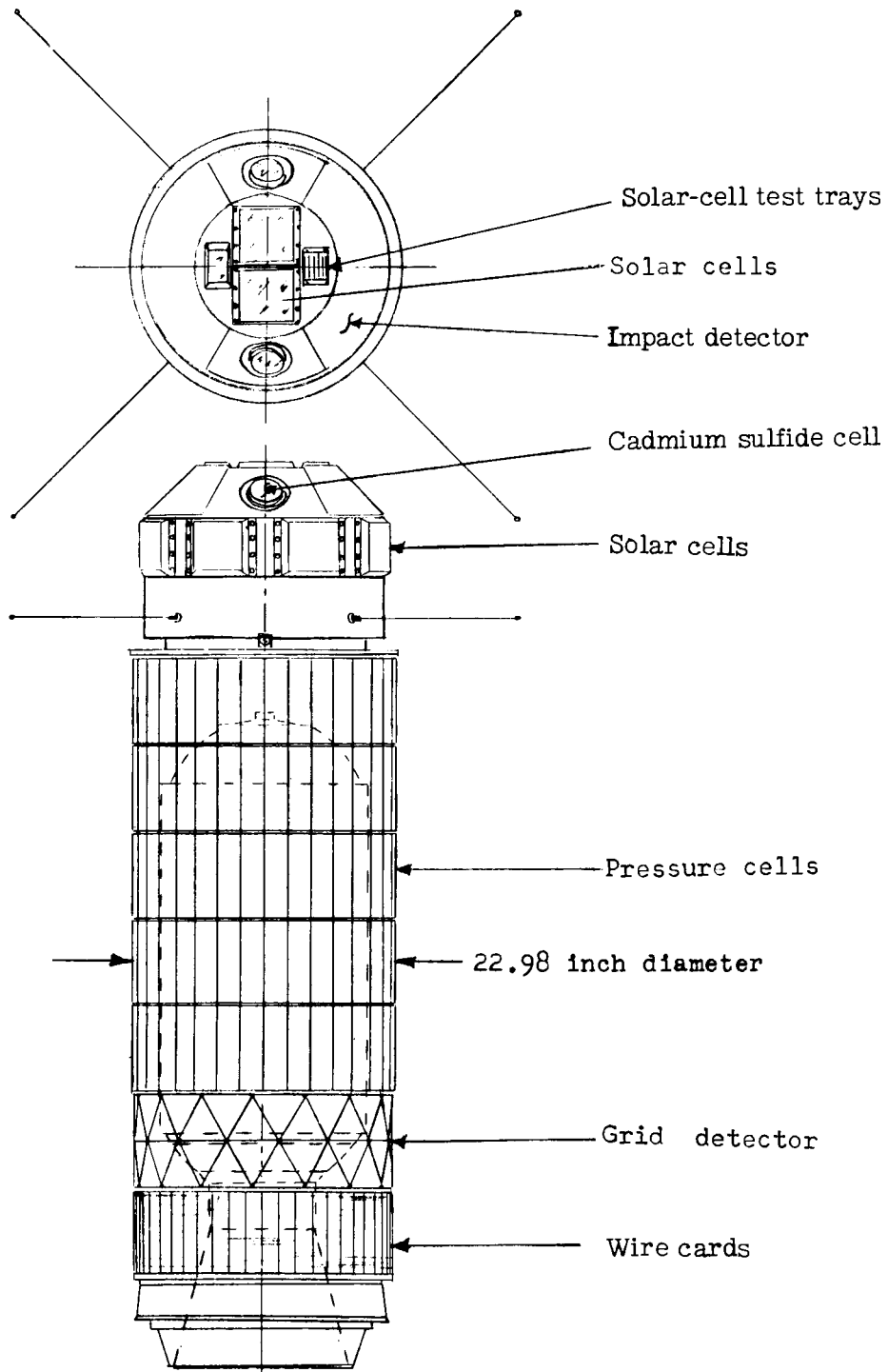
(a) Two-view drawing of satellite.

Figure 1.- The Explorer XVI satellite.
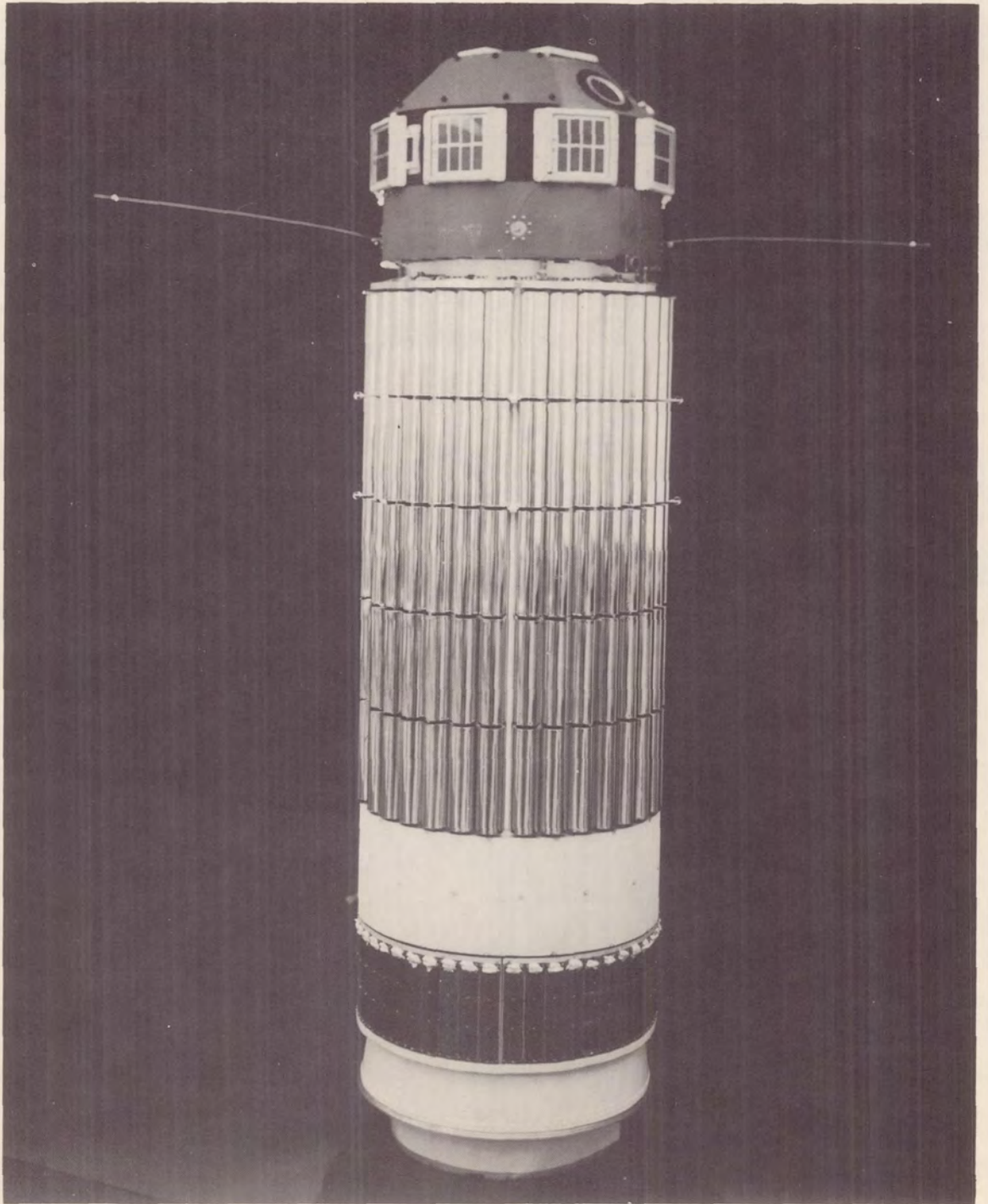
(b) Photograph of satellite.   L-62-6995

Figure 1.- Concluded.

Pinch-off tube

Test material

7.40

.12

Mounting bracket

1.46

A-A

Pressure sensitive
capsule

Plunger

Base plate

.97 rad.

Microswitch

Switch actuation adjustment cam
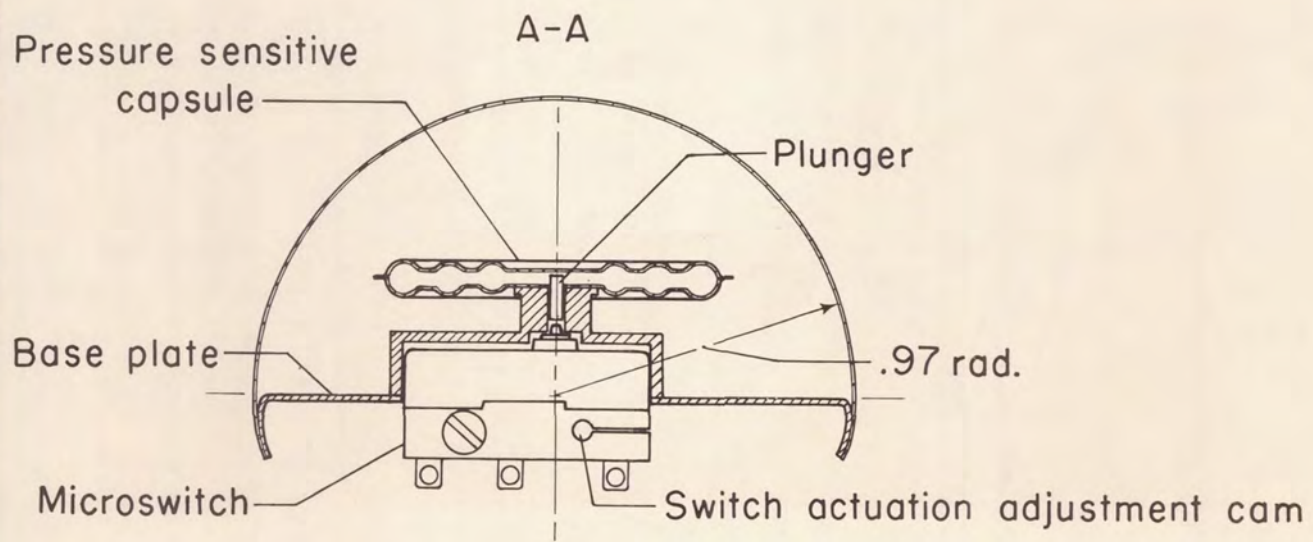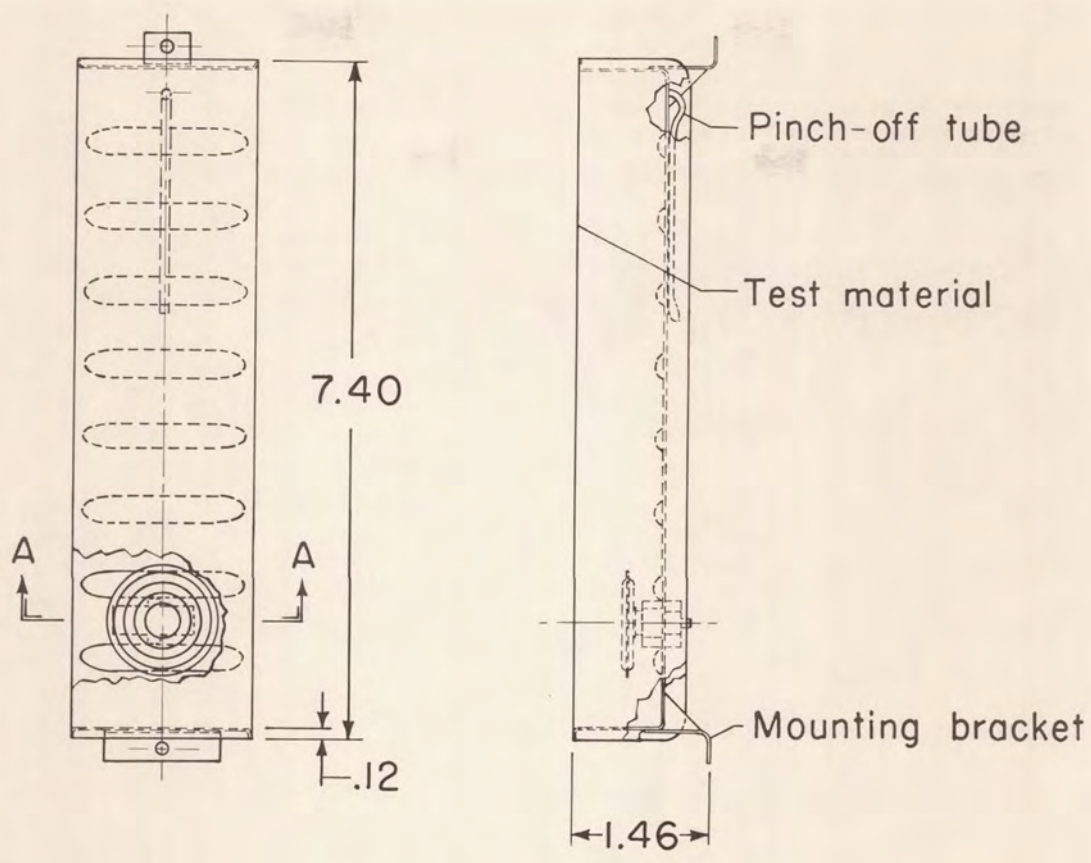
Figure 2.- Pressurized-cell detector. All dimensions are in inches.

Figure 3.- Mounting arrangement of pressurized cells. All dimensions are in inches.

0.036

0.002

0.002

0.002

0.006

Gold grid dimensions

0.12

60°

4.57

0.001-, 0.003-, or 0.006-thick stainless-
steel cover

0.0005-thick Mylar insulator

0.000060-thick gold grid

0.25 polyurethane foam
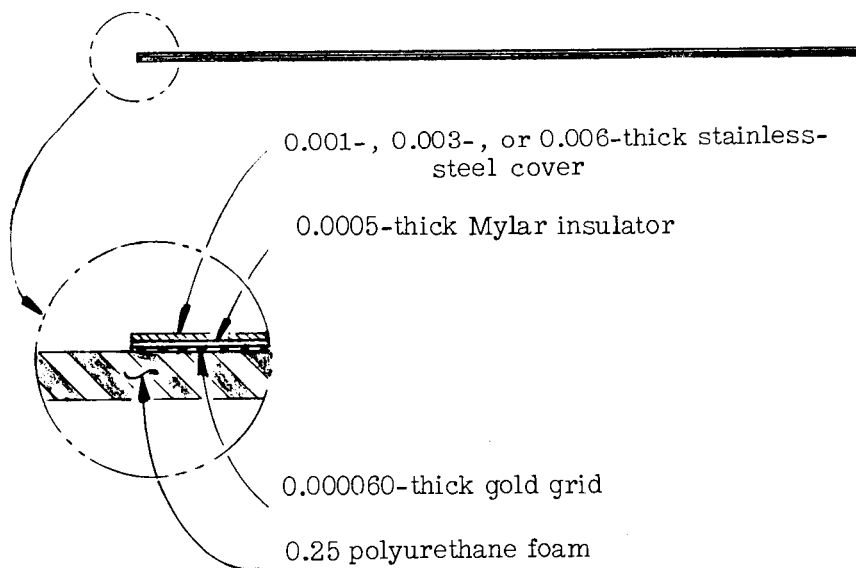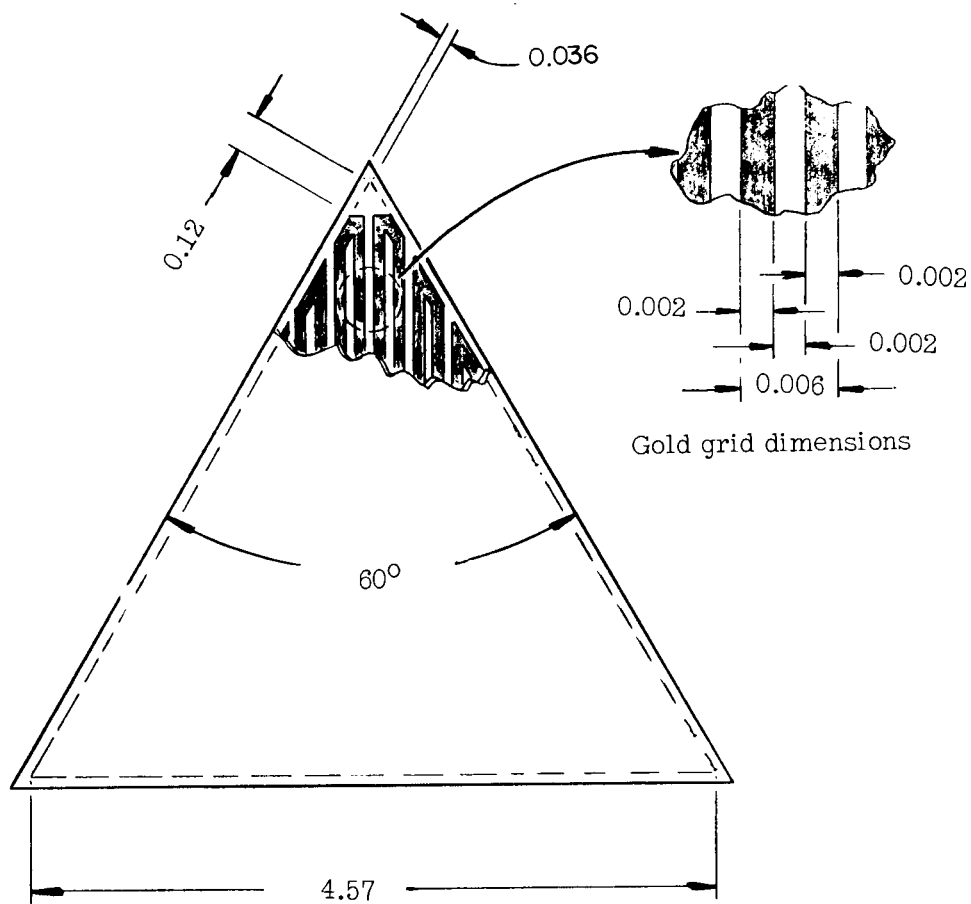
Figure 4.- Stainless-steel-covered grid detector. All dimensions are in inches.

0.032-thick
melamine laminate

7.00

1.45

0.002- or 0.003-diameter enameled
copper wire winding

300 Ω
resistor

100 Ω
thermistor

Copper terminal
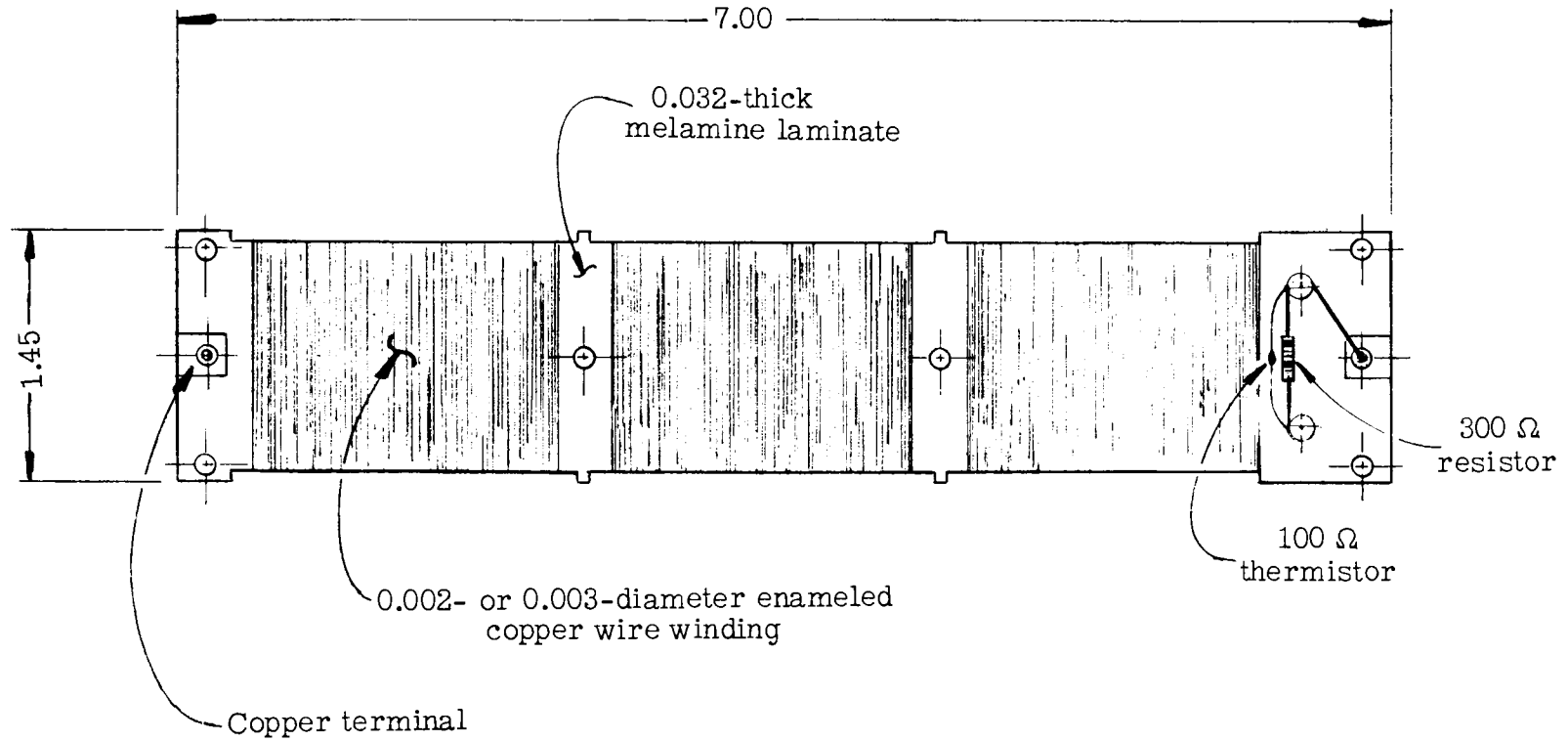
Figure 5.- Copper-wire card detector. All dimensions are in inches.
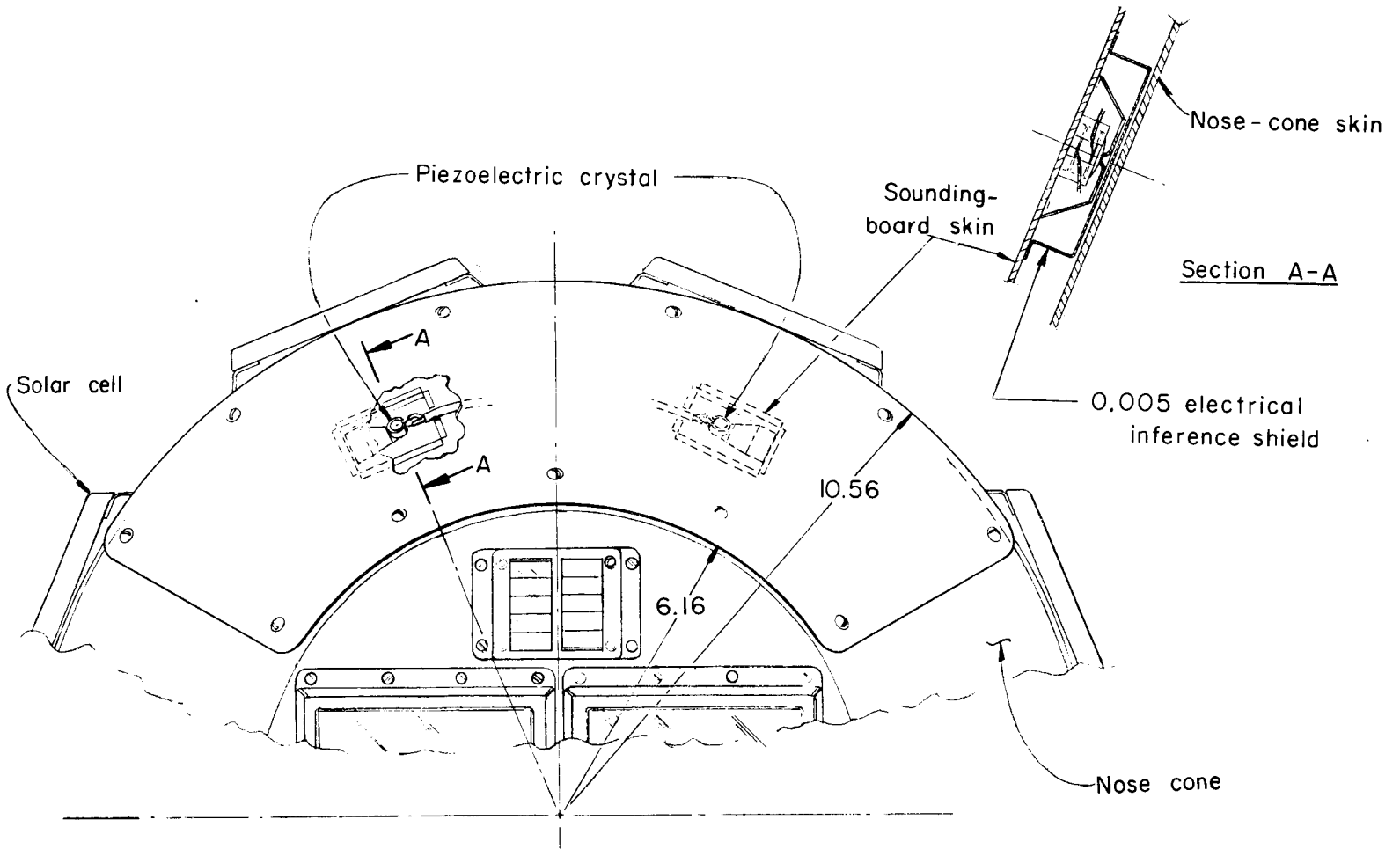
Figure 6.- Sounding-board impact detectors.   All dimensions are in inches.

7.40

1.94

Pressurized cell showing location
of impact detector

Cantilever spring
holding clip

Brass dome

Mica insulator

Electrical contact

Lead zirconate titanate
piezoelectric element

Quartz transfer disc

Plastic positioning ring
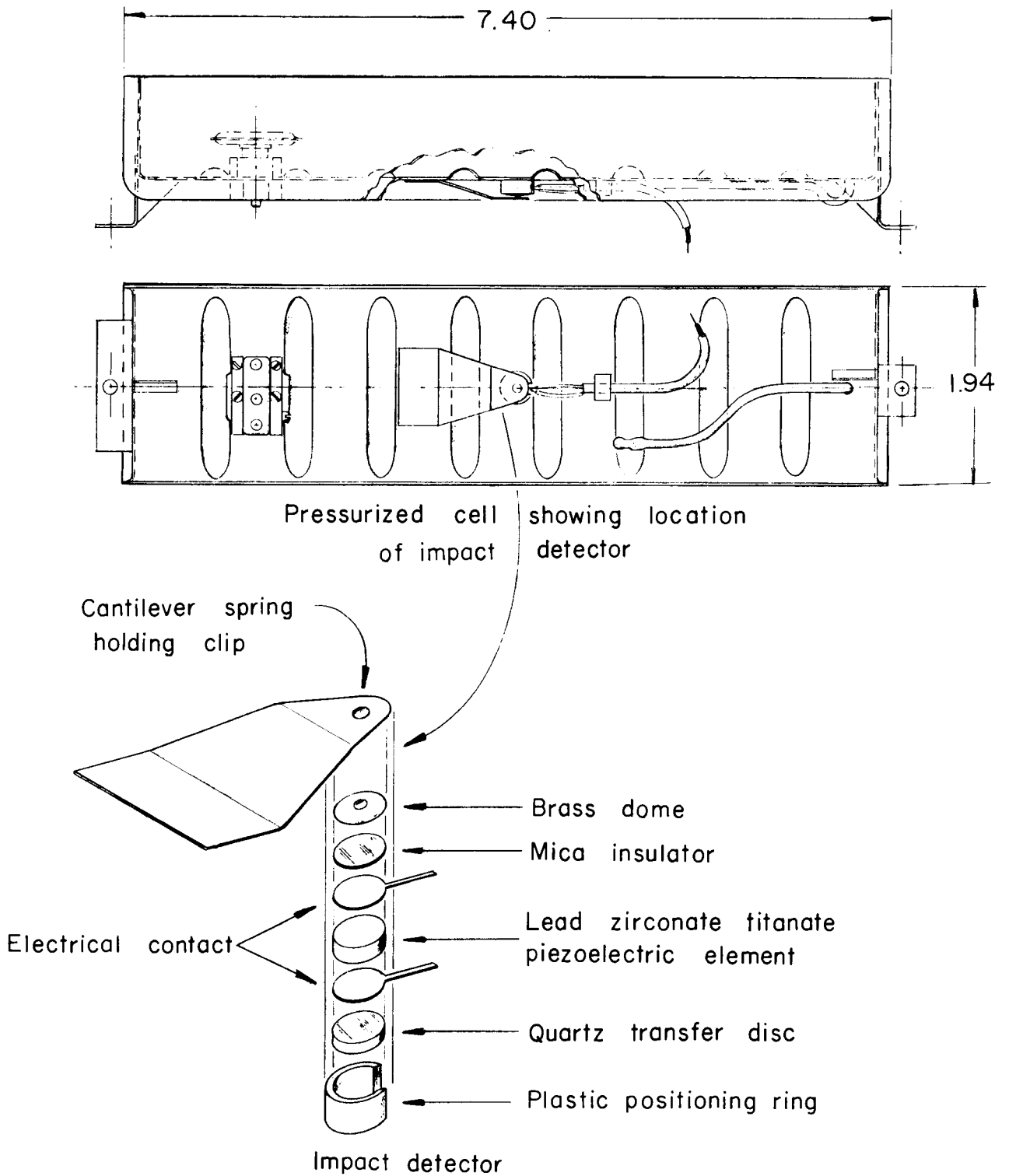
Impact detector

Figure 7.- Impact detector mounted on pressurized cell.   All dimensions are in inches.
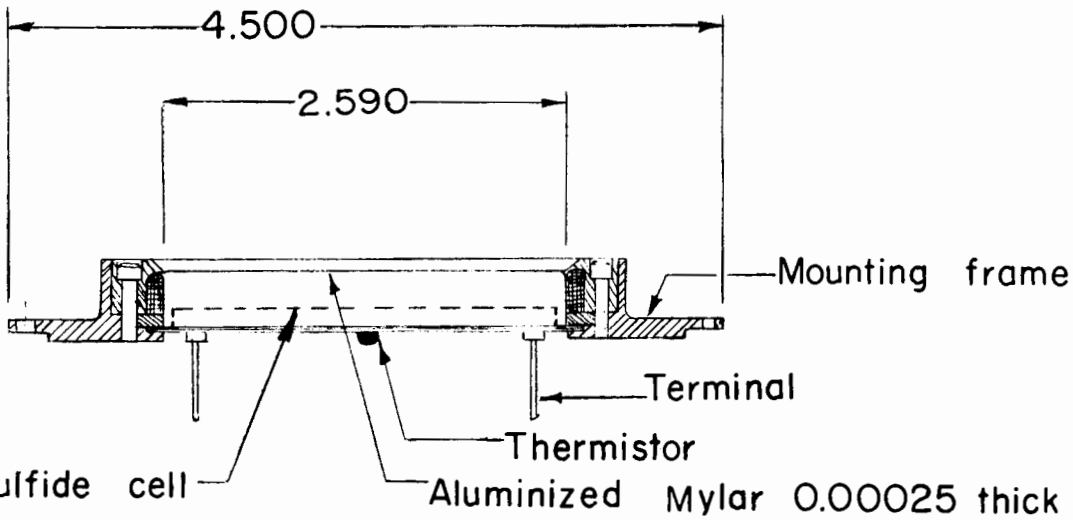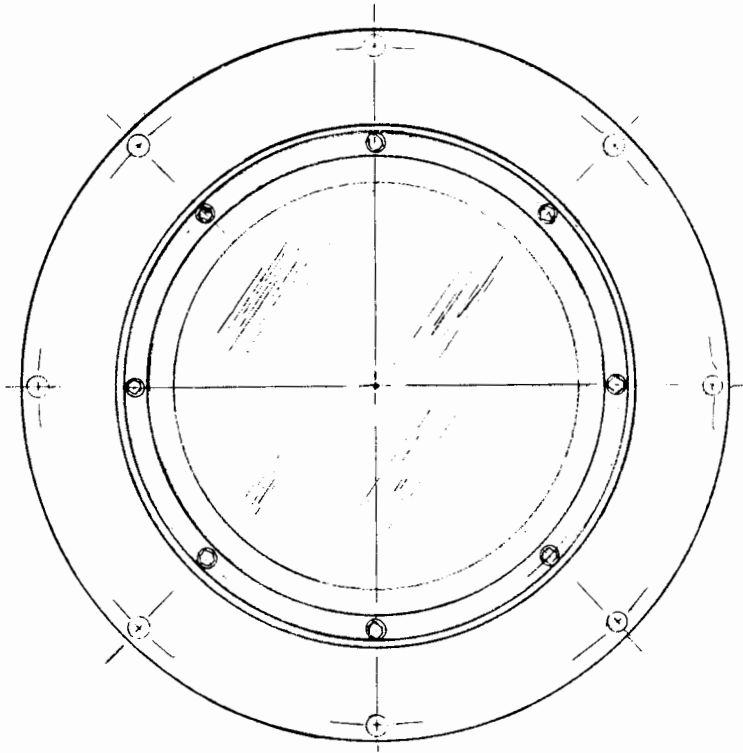
Figure 8.- Cadmium sulfide cell. All dimensions are in inches.
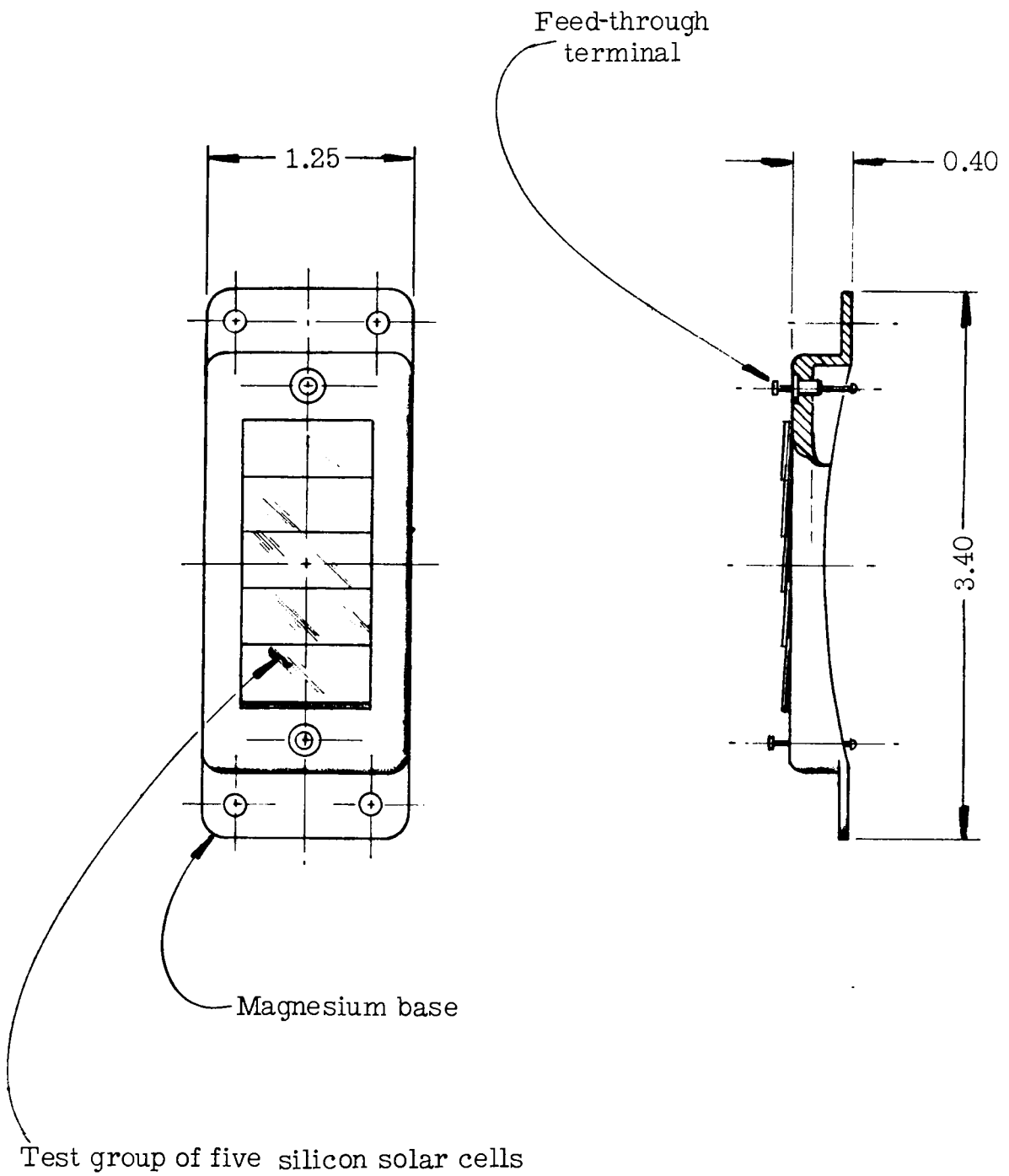
Figure 9.- Test solar-cell group.   All dimensions are in inches.
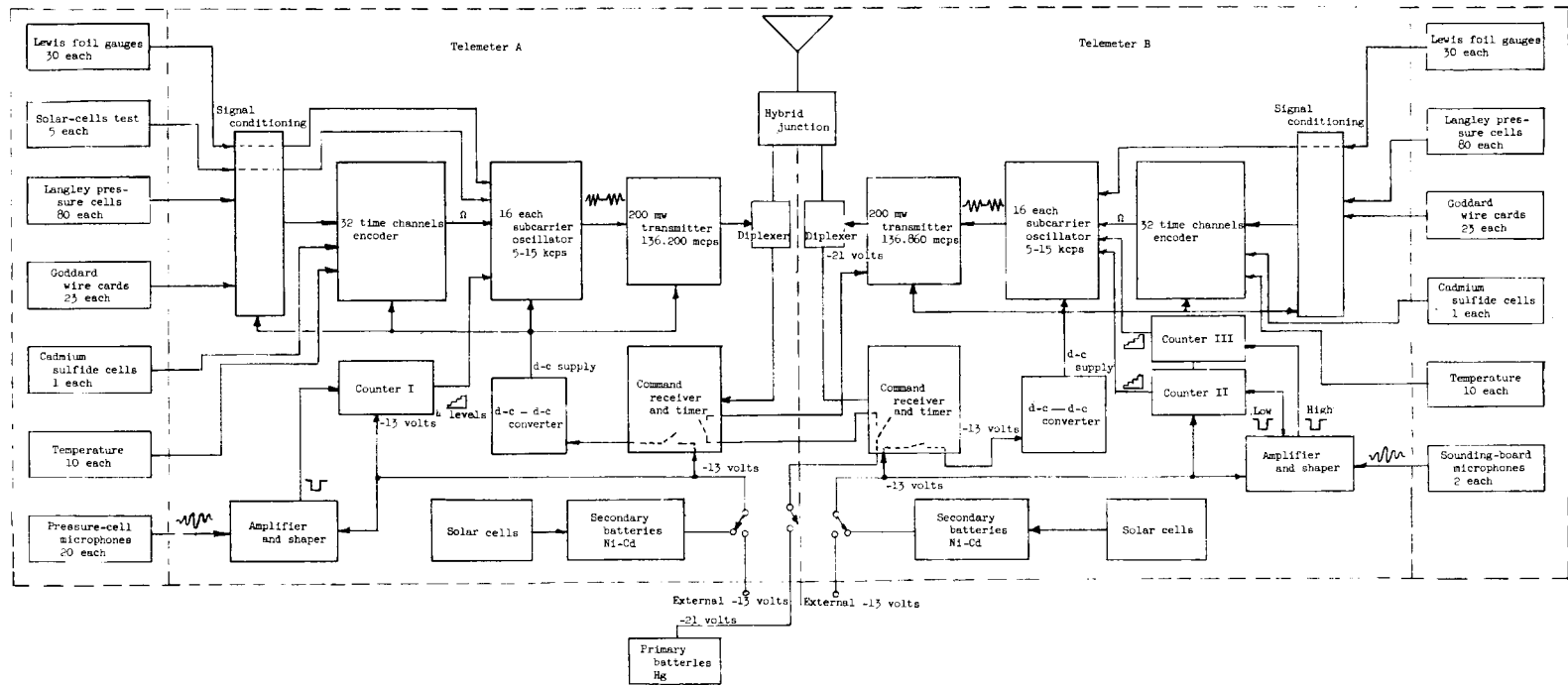
Figure 10.- Block diagram of telemeters.
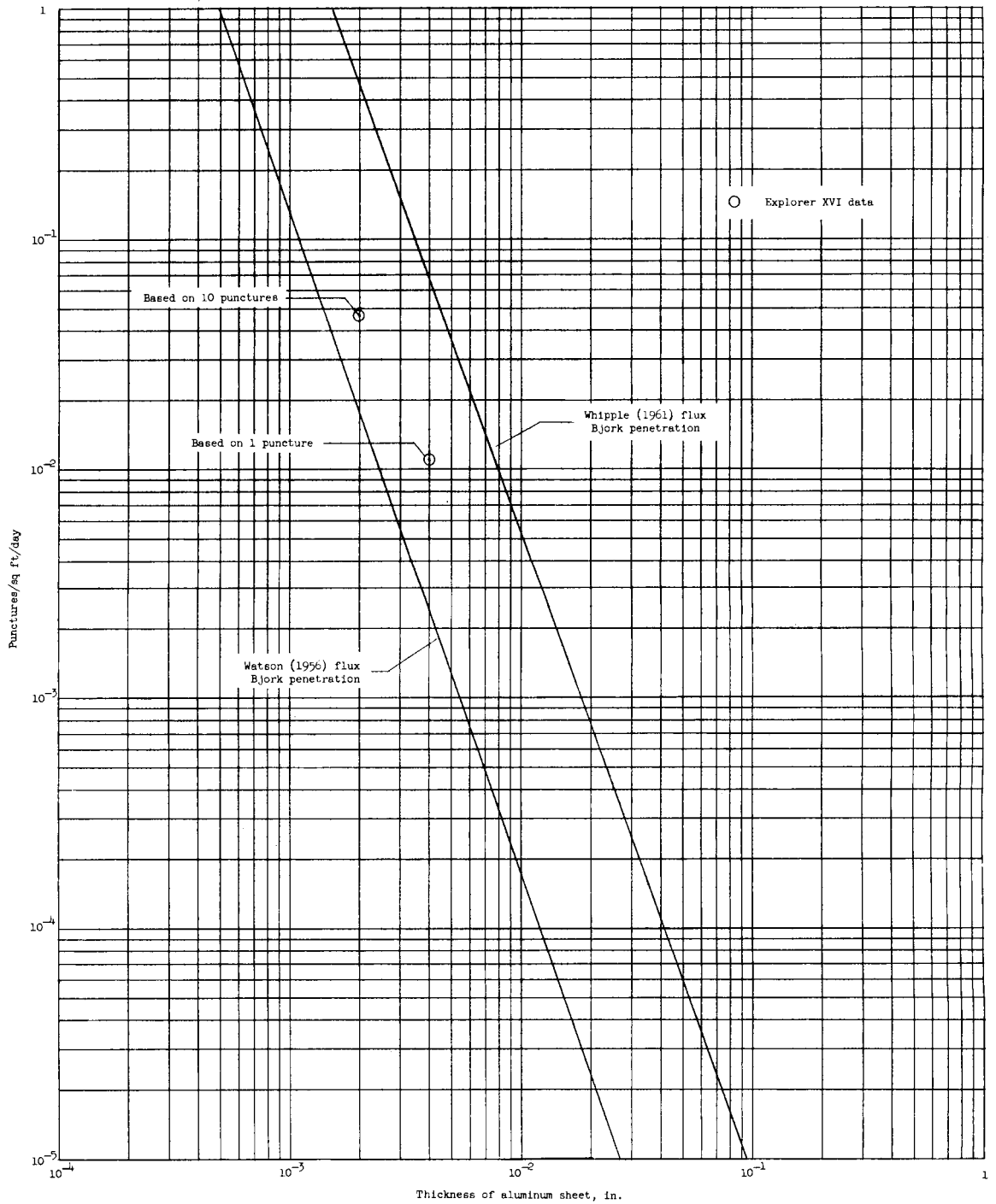
Figure 11.- Most probable rate of puncture of aluminum skin as a function of skin thickness, based on application of Bjork penetration theory to Whipple (1961) and Watson (1956) fluxes (assuming meteoroid density of 2.7 g/cu cm). Circles represent data from beryllium-copper pressure cells on Explorer XVI, as of January 13, 1963, tentatively interpreted in terms of aluminum.
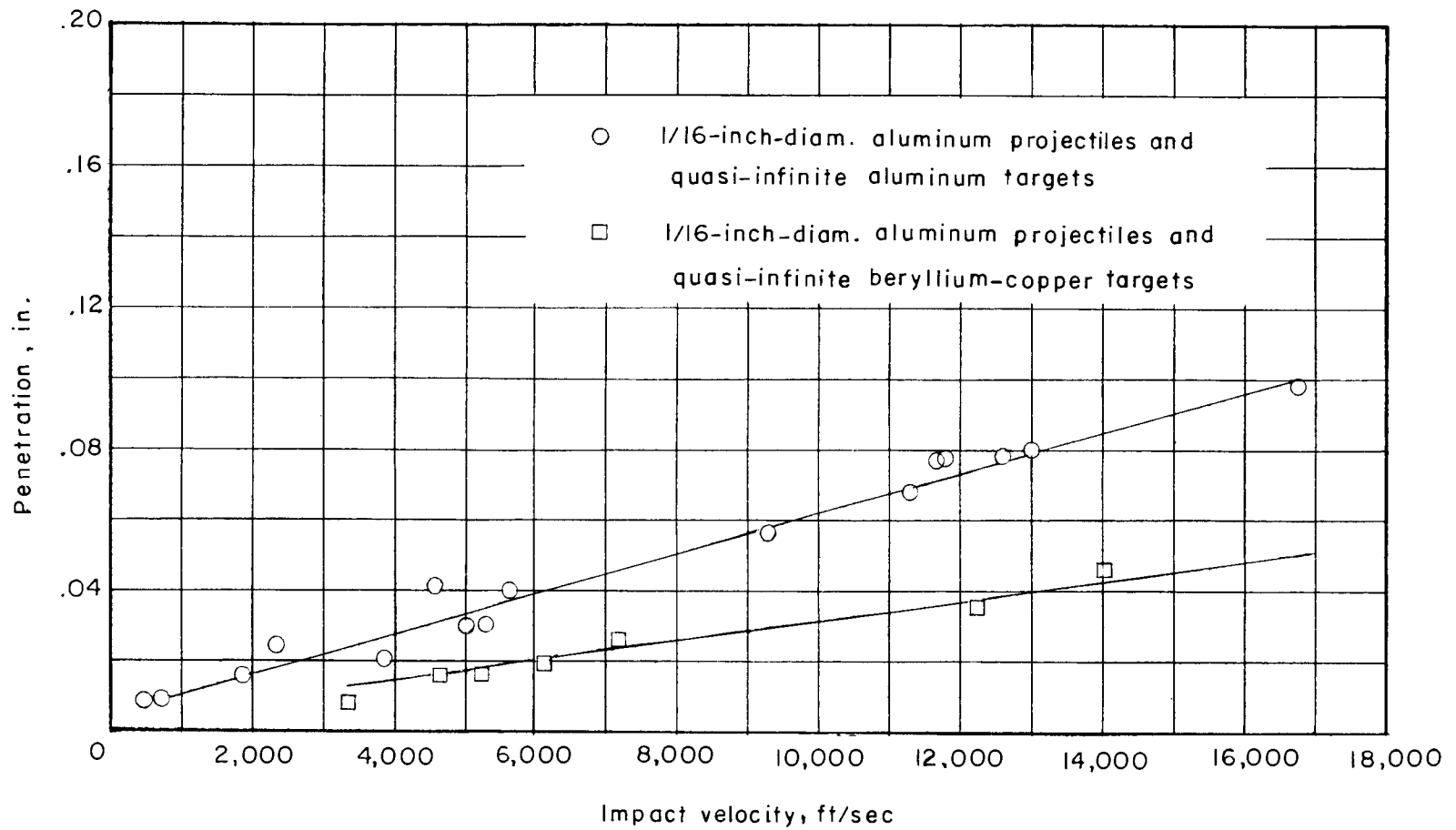
Figure 12.- Comparison of penetration in aluminum and beryllium-copper targets.
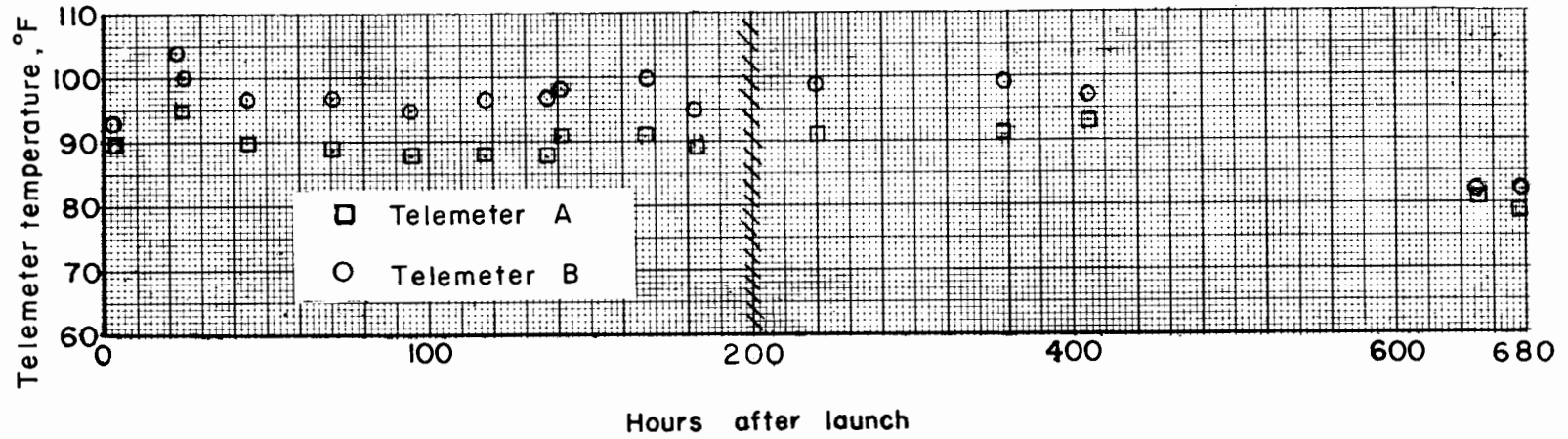
Figure 13.- Variation of telemeter temperature with time after launch. Note change in scale after 200 hours.